

1 **Empowering a mesophilic inoculum for thermophilic nitrification: growth mode and**
2 **temperature pattern as critical proliferation factors for archaeal ammonia oxidizers**

3

4 Emilie N. P. Courtens¹, Tom Vandekerckhove¹, Delphine Prat¹, Ramiro Vilchez-Vargas¹,
5 Marius Vital², Dietmar H. Pieper², Ken Meerbergen³, Bart Lievens³, Nico Boon^{1*} and
6 Siegfried E. Vlaeminck^{1,4,*}✉

7

8 ¹Laboratory of Microbial Ecology and Technology (LabMET), Ghent University, Coupure Links 653, 9000
9 Gent, Belgium

10 ²Microbial Interactions and Processes Research Group, Helmholtz Centre for Infection Research, Braunschweig,
11 Germany

12 ³Laboratory for Process Microbial Ecology and Bioinspirational Management (PME&BIM), KU Leuven,
13 Campus De Nayer, Fortsesteenweg 30A, 2860 Sint-Katelijne-Waver, Belgium

14 ⁴Research Group of Sustainable Energy, Air and Water Technology, Department of Bioscience Engineering,
15 University of Antwerp, Groenenborgerlaan 171, 2020 Antwerpen, Belgium

16

17 *These authors contributed equally and are both senior authors for this work

18 ✉ Corresponding author: Siegfried E. Vlaeminck

19 Tel.: +32-9-2645976

20 Fax: +32-9-2646248

21 E-mail: siegfried.vlaeminck@UGent.be

22

23 **Keywords: Archaea, thermophile, *Nitrospira*, *Nitrososphaera***

24 **Abstract**

25

26 Cost-efficient biological treatment of warm nitrogenous wastewaters requires the
27 development of thermophilic nitrogen removal processes. Only one thermophilic nitrifying
28 bioreactor was described so far, achieving $200 \text{ mg N L}^{-1} \text{ d}^{-1}$ after more than 300 days of
29 enrichment from compost samples. From the practical point of view in which existing plants
30 would be upgraded, however, a more time-efficient development strategy based on
31 mesophilic nitrifying sludge is preferred. This study evaluated the adaptive capacities of
32 mesophilic nitrifying sludge for two linear temperature increase patterns (non-oscillating vs.
33 oscillating), two different slopes (0.25 vs. $0.08 \text{ }^\circ\text{C d}^{-1}$) and two different reactor types (floc vs.
34 biofilm growth). The oscillating temperature pattern ($0.25 \text{ }^\circ\text{C d}^{-1}$) and the moving bed biofilm
35 reactor ($0.08 \text{ }^\circ\text{C d}^{-1}$) could not reach nitrification at temperatures higher than 46°C . However,
36 nitrification rates up to $800 \text{ mg N L}^{-1} \text{ d}^{-1}$ and $150 \text{ mg N g}^{-1} \text{ volatile suspended solids d}^{-1}$ were
37 achieved at a temperature as high as 49°C by imposing the slowest linear temperature increase
38 to floccular sludge. Microbial community analysis revealed that this successful transition was
39 related with a shift in ammonium oxidizing archaea dominating ammonia oxidizing bacteria,
40 while for nitrite oxidation *Nitrospira* spp. was constantly more abundant than *Nitrobacter*
41 spp.. This observation was accompanied with an increase in observed sludge yield and a shift
42 in maximal optimum temperature, determined with ex-situ temperature sensitivity
43 measurements, predicting an upcoming reactor failure at higher temperature. Overall, this
44 study achieved nitrification at 49°C within 150 days by gradual adaptation of mesophilic
45 sludge, and showed that ex-situ temperature sensitivity screening can be used to monitor and
46 steer the transition process.

47 **1. Introduction**

48 The extensive production of inorganic nitrogen fertilizers is crucial to sustain food production
49 for the increasing global population and living standard (Erisman et al. 2008). This, however,
50 resulted in the accumulation of reactive nitrogen species in many natural ecosystems, causing
51 a worldwide environmental problem (Galloway et al. 2014). Ammonia nitrogen is a major
52 wastewater component inducing eutrophication and fish mortality when released in water
53 bodies without prior treatment (Camargo and Alonso 2006). Nitrification, the microbial
54 oxidation of ammonium to nitrate, plays a key role in the initial transformation of reactive
55 nitrogen in wastewater treatment. Aerobic ammonium-oxidizing bacteria (AOB) and archaea
56 (AOA) catalyze the first, rate-limiting step, i.e. oxidation of ammonium (NH_4^+) to nitrite
57 (NO_2^-) (also known as nitritation), while the successive oxidation to nitrate (NO_3^-) (also
58 referred to as nitrataion), is usually carried out by aerobic nitrite-oxidizing bacteria (NOB).
59 Nitrification is conventionally followed by the reductive denitrification process to achieve
60 complete nitrogen removal, although short-cut nitrogen removal processes, such as partial
61 nitritation/anammox (PN/A), are gaining importance over the last years (Lackner et al. 2014,
62 Vlaeminck et al. 2012).

63 Although nitrification is an established biological process to treat ammoniacal wastewater,
64 applications above 40°C still represent a significant challenge. The development of
65 thermophilic nitrification could enable the treatment of warm wastewaters, such as hot
66 industrial wastewater and thermophilic anaerobic digester supernatant, without the need of
67 additional cooling and thus lower both the capital as operational costs. Experiences with
68 carbon treatment, moreover, suggest that a more stable process with higher specific rates
69 (smaller bioreactors), a lower sludge production and a lower level of contamination could be
70 achieved at thermophilic conditions (Lapara and Alleman 1999). Thermophilic nitrogen

71 removal would, thus, not only be a sustainable and an economically favorable solution for the
72 treatment of warm wastewaters, but also for wastewaters on sites with excess available heat.

73 Two fundamentally different strategies can be used to achieve thermophilic nitrification for
74 wastewater treatment, including a strategy based on a thermophilic nitrifying inoculum or
75 based on a mesophilic community which has been adapted to higher temperatures. As both
76 thermophilic AOA (e.g. “*Candidatus Nitrosocaldus yellowstonii*”, “*Candidatus*
77 *Nitrososphaera gargensis*”) and NOB (e.g. *Nitrospira calida*) have been separately enriched
78 from terrestrial hot springs, respective environmental samples may serve as inoculum to
79 enrich a thermophilic nitrifying community (de la Torre et al. 2008, Hatzenpichler et al. 2008,
80 Lebedeva et al. 2011). Indeed, Courtens et al. (*Under review*) recently showed the enrichment
81 of autotrophic thermophilic nitrifiers from compost samples and the successful operation of a
82 thermophilic nitrifying bioreactor at 50°C with biotechnological potential. However, the low
83 growth rate and/or low relative abundance of those thermophilic autotrophs in environmental
84 samples may result in very long and laborious enrichment processes, which may impede the
85 upgrade of existing wastewater treatment plants. From a practical point of view the second
86 strategy, in which existing mesophilic nitrifying communities are adapted to elevated
87 temperatures, may thus be more appropriate. Shore et al. (2012) achieved complete
88 nitrification at 40°C applying a stepwise temperature increase from 30 to 40°C (10°C d⁻¹) to a
89 moving bed biofilm reactor (MBBR). In a parallel MBBR the temperature was increased from
90 30 to 45°C (15°C d⁻¹), however, losing all nitrifying activity. Slightly higher nitrification
91 temperatures (42.5°C) were reached by Courtens et al. (2014a) who imposed smaller
92 temperature differences (2.5°C d⁻¹) from 40°C on. It was furthermore demonstrated that salt
93 amendment can be used as a tool to reach more efficient temperature transitions. However,
94 from those studies it is clear that no ‘real’ thermophilic (>45°C) nitrification can be achieved
95 through a stepwise temperature increase pattern (> 2.5°C d⁻¹), although short-term activity

96 measurements of mesophilic sludge (34°C) showed nitrifying potential up to 50°C (Lopez-
97 Vazquez et al. 2014).

98 Therefore, in this study, the adaptive capacities of mesophilic nitrifying sludge to gradual
99 temperature increase patterns were explored. In a first reactor experiment, a non-oscillating
100 linear temperature increase ($0.25^{\circ}\text{C d}^{-1}$) was compared with an oscillating increase (amplitude
101 2°C) with the same final slope. Pre-exposure to a certain stress can in some cases result in an
102 increased resilience towards this stress as shown for copper stress in denitrifiers (Li et al.
103 2014, Philippot et al. 2008). In a second experiment, a linear temperature increase with a
104 lower slope ($0.08^{\circ}\text{C d}^{-1}$) was investigated, in which a floccular growth system (SBR) was
105 compared with a biofilm based system (MBBR). Biomass retention of the slow growing
106 thermophilic autotrophs is essential, and could eventually be favored through a biofilm based
107 reactor system. Finally, the nitrifying community was closely monitored by batch activity
108 tests and molecular analyses during the linear temperature increase to elucidate the adaptation
109 process or shifts in the microbial community.

110 2. Materials and methods

111 2.1. Reactor set-up and operation

112 An overview of the two reactor experiments and associated reactor parameters is presented in
113 **Table 1**. In the first experiment with two identical lab-scale sequential batch reactors (SBR), a
114 linear temperature increase ($0.25^{\circ}\text{C d}^{-1}$) with (SBR₁) and without (SBR₂) an oscillation
115 (amplitude 2°C , frequency 0.088 d^{-1}) were compared. In the second reactor experiment, a
116 lower linear temperature increase ($0.08^{\circ}\text{C d}^{-1}$) was applied, and a SBR (SBR₃) was compared
117 with a MBBR. The majority of the process and feeding parameters were the same in all
118 reactors to investigate the effect of temperature pattern and/or sludge aggregation (flocs
119 versus biofilm) (**Table 1**).

120 The reactor vessels (working volume 2 L, diameter 12 cm) were jacketed, allowing
121 temperature control with a circulating thermostatic water bath, and equipped with a stirring
122 device. The reactor pH was controlled between pH 6.5 and 7.5 by dosage of 0.1 M
123 NaOH/HCl, and continuous aeration was provided by air pumps through a diffuser stone. The
124 synthetic medium consisted of $(\text{NH}_4)_2\text{SO}_4$ ($10\text{-}800 \text{ mg N L}^{-1}$), $11\text{-}12 \text{ g NaHCO}_3 \text{ g}^{-1} \text{ N}$,
125 KH_2PO_4 (10 mg P L^{-1}) and 0.1 mL L^{-1} trace element solution dissolved in tap water (Kuai and
126 Verstraete 1998). The nitrogen loading was adjusted through the ammonium concentration in
127 the influent. The 6- and 4-h cycle of the SBR consisted of a 330 and 210-min aerobic reaction
128 period including three 25-min feeding periods, a 15-min settling period, a 5-min decanting
129 period and a 10-min idle period.

130 The carrier material of the MBBR consisted of polyvinyl alcohol (PVA)-gel beads (Kuraray,
131 Japan) at a volumetric filling ratio of 15%. All reactors were inoculated with the same
132 commercial nitrifying inoculum (Avecom NV, Ghent, Belgium) at an initial biomass
133 concentration of $2.4 \pm 0.1 \text{ g volatile suspended solids (VSS) L}^{-1}$. To ensure sufficient biomass

134 growth on the carriers of the MBBR, a stabilization period (79 days) was included in the
135 second experiment. The MBBR was initially operated in the same sequencing batch
136 feeding/withdrawal mode during the stabilization period to ensure enough suspended biomass
137 for biomass growth on the carriers. Once growth was observed on the carriers, initially, half
138 of the suspended biomass was wasted (day 23 of the stabilization period). Further on, the
139 residual suspended biomass was gradually wasted at about 45 mg VSS d⁻¹ until day 79 when
140 the settling period was excluded.

141 **2.2. Ex-situ nitrification activity tests**

142 In parallel with the second reactor experiment, batch activity tests were performed with the
143 SBR₃ sludge and MBBR carriers to monitor the progress of the optimal temperature for both
144 ammonia and nitrite oxidation. Temperature sensitivity measurements were performed at
145 reactor temperatures of 38°C, 40°C, 42°C, 44°C, 46°C and 48°C, in which the specific
146 ammonia and nitrite oxidizing activities were measured at the respective reactor temperature
147 ±2°C. For the SBR₃ sludge, 96-well plates with a working volume of 250 µL were used, while
148 the MBBR carriers were transferred in 24-well plates with a working volume of 1.5-2.5 mL.
149 Plates were incubated in a MB100-4A Thermoshaker (Hangzhou Allsheng Instruments,
150 China) at the specific temperature, in which oxygen was provided through intensive shaking
151 at 600 rpm. The buffer solution (pH 7) contained final concentrations of 2 g P L⁻¹
152 (KH₂PO₄/K₂HPO₄), 1 g NaHCO₃ L⁻¹ and 60 mg N L⁻¹ ((NH₄)₂SO₄ or NaNO₂). The sensitivity
153 of ammonia and nitrite oxidation for free ammonia (FA) was also evaluated by determining
154 the specific activity at different ammonium concentrations (25-200 mg N L⁻¹). All treatments
155 were performed in sextuple, and liquid samples (2 µL) were taken over time for NH₄⁺ and
156 NO₂⁻ analysis. These high-throughput activity measurements were highly optimized for each
157 sludge type prior to the actual tests, demonstrating no oxygen limitation as increased shaking
158 speed (250-600 rpm) did not increase nitrogen oxidation rates. A validation experiment was

159 performed in which the obtained rates were not significantly different with rates obtained in
160 conventional 250 mL Erlenmeyer aerobic batch tests without oxygen limitation as monitored
161 with an online DO measurement (Windey et al. 2005).

162 **2.3. Sludge production and settleability**

163 Sludge production was evaluated through the observed sludge yield (Y), calculated using
164 cumulative terms, as described previously (Courtens et al. 2014b). Biomass settleability of the
165 floccular sludge was measured through the determination of the sludge volume index (SVI) in
166 a 1 L Imhoff cone, with the sludge height variation monitored for 5 min instead of 30 min to
167 prevent extensive cooling of the sludge.

168 **2.4. Molecular analyses**

169 Biomass samples (± 2 g) of the inoculum and the reactors (SBR₃ and MBBR) were collected
170 over time, and total DNA was extracted using the Fast-Prep24 instrument (MP-BIO,
171 Germany) as described previously (Vilchez-Vargas et al. 2013). DNA quality and quantity
172 were analysed electrophoretically on 1% (w/v) agarose gel and spectrophotometrically by
173 determination of the absorbance ratios at 260 nm and 280 nm and the absorbance at 260nm,
174 using a NanoDrop ND-1000 instrument (Thermo Scientific), respectively. Abundance of the
175 16S ribosomal RNA (rRNA) genes of *Nitrospira* spp. and *Nitrobacter* spp. and the functional
176 gene encoding the A subunit of the bacterial and archaeal monooxygenase (*amoA*) was
177 monitored using quantitative PCR (qPCR) assays on an ABI StepOnePlus real-time PCR
178 instrument (Life Technologies, Carlsbad, CA, USA). Whereas *amoA* abundance is a good
179 proxy for monitoring AOB and AOA abundance, the genera *Nitrospira* and *Nitrobacter*
180 represent major NOB. Reactions were performed in a total volume of 20 μ l consisting of 10 μ l
181 of iTaq Universal SYBR Green Supermix (Bio-Rad Laboratories, Hercules, CA, USA), 1.0 μ l
182 DNA template (diluted), 0.3 (*Nitrobacter*), 0.5 (*amoA*) or 0.6 μ l (*Nitrospira*) of each forward

183 and reverse primer, adjusted to a final volume of 20 μ l with H₂O (Table S1). Amplifications
184 were run as follows: initial denaturation for 2 min at 95 °C followed by 40 cycles of 15 s
185 denaturation at 94 °C, 30 s annealing at the temperature mentioned in Table S1 (supplemental
186 information) and 30 s elongation at 60 °C. Each sample extract was amplified in triplicate and
187 target quantification was performed using a standard curve. Standard curves (range: 1.0E+02 -
188 1.0E+07 copies μ l⁻¹) were generated using six ten-fold dilutions of target DNA from
189 Fosmid54D9 (Treusch et al. 2005), *Nitrosomonas europaea* DSM 28437, *Nitrobacter*
190 *winogradskyi* DSM 10237 and *Nitrospira moscoviensis* DSM 10035. Additional
191 positive/negative controls and a melting curve analysis were performed in all analyses to
192 verify target specific amplification, the absence of contaminants, and to confirm product
193 specificity, respectively.

194 The overall community structure was analyzed using paired-end high-throughput sequencing
195 (MiSeq Illumina platform) of amplified V5-V6 regions of the 16S rRNA gene, using the
196 universal primers 807F and 1050R (Bohorquez et al. 2012). Amplification, library
197 preparations, sequencing and bioinformatic processing of sequences was done according to
198 Camarinha-Silva et al. (2014) with some modifications. Prior to the addition of barcodes and
199 Illumina adapters the template was enriched by 20 PCR cycles using primers 807F and
200 1050R. Raw sequences were assembled (Cole et al. 2014) and subsequently aligned using
201 MOTHUR (gotoh algorithm with the SILVA reference database) prior to preclustering
202 allowing two mismatches (Schloss et al. 2009). Next, sequences were clustered at a sequence
203 similarity cut-off value of 99% to define species-level operational taxonomic units (OTUs).
204 Only OTUs (phylotypes,Phy) exhibiting an average abundance of at least 0.001% of the total
205 communities and a sequence length >200bp were considered for further analysis.
206 Phylogenetic analyses were performed with MEGA5 (Tamura et al. 2011) using the neighbor-
207 joining method with Jukes-Cantor correction and pairwise deletion of gaps/missing data. A

208 total of 1000 bootstrap replications were performed to test for branch robustness. A heat map
209 was generated using gplots and RColorBrewer packages.

210

211 **2.5. Chemical analyses**

212 Ammonium (Nessler method), total suspended solids (TSS) and volatile suspended solids
213 (VSS) were measured according to standard methods (Greenberg et al. 1992). The biomass
214 concentration in the MBBR was determined through extraction of the biomass from the PVA
215 carriers and subsequent protein measurement. The protein content was then translated to a
216 VSS concentration using the average protein content of the MBBR sludge, $0.31 \text{ g protein g}^{-1}$
217 $\text{VSS}_{\text{MBBR sludge}}$ as determined. The carriers were cut in fine pieces and incubated in 1 M NaOH
218 for 2 hours at 46°C with regular mixing for biomass extraction. To determine the protein
219 concentration in the extract, the method developed by Lowry was used with bovine serum
220 albumin (BSA) as the standard (Lowry et al. 1951). Nitrite and nitrate were determined on a
221 930 Compact Ion Chromatograph (Metrohm, Switzerland), equipped with a conductivity
222 detector. Dissolved oxygen (DO) and pH were measured with an HQ30d DO meter (Hach
223 Lange, Germany) and a Dulcotest pH-electrode PHEP 112 SE (Prominent, Germany),
224 respectively. In the batch activity tests, the liquid samples for ammonium and nitrite
225 determination were always immediately analyzed spectrophotometrically with the Berthelot
226 and Montgomery reaction, including a triplicate standard curve for each analysis run.
227 Measurements were obtained using a Tecan infinite plate reader (Tecan, Switzerland), and
228 biomass was quantified through protein concentrations.

229

230 **3. Results**

231 **3.1. Oscillating versus non-oscillating linear temperature increase**

232 The adaptive capacities of mesophilic nitrifying sludge were first evaluated for two different
233 gradual temperature increase patterns. An oscillating temperature increase with an amplitude
234 of 2°C and a frequency of 0.088 d⁻¹ was compared with a non-oscillating increase with the
235 same linear slope (0.25°C d⁻¹) as shown in **Figure 1**. Prior to any temperature increase, the
236 reactors were started up identically at 37°C reaching ammonium removal rates of 180 ± 14
237 mg N L⁻¹ d⁻¹ or 136 ± 10 mg N g VSS⁻¹ d⁻¹ after one week of stabilization. Nitrite
238 accumulation was negligible in both reactors and nitrate production accounted for 95% of the
239 ammonium removal. Up to 40°C, no changes in volumetric ammonium removal rates were
240 observed in both reactors. Further temperature increase above 40°C, however, negatively
241 affected the nitrifying activity in both reactors, with a more pronounced effect in the
242 oscillating reactor. At 42°C, only 15% of the initial volumetric nitrifying activity remained in
243 the oscillating reactor (26 ± 5 mg N L⁻¹ d⁻¹) while 50% remained in the non-oscillating one
244 (90 ± 3 mg N L⁻¹ d⁻¹) (**Figure 1**). Although the non-oscillating reactor seemed to better resist
245 the temperature increase, the decreasing trend pursued in both reactors finally resulting in an
246 entire loss of activity at 45°C in both reactors, suggesting that the imposed slope of 0.25°C d⁻¹
247 was too high.

248 **3.2. Floccular versus biofilm based reactor system**

249 **3.2.1. Reactor performance**

250 In the second reactor experiment, a linear temperature increase with a lower slope was
251 investigated (0.08-0.16°C d⁻¹), in which a SBR (SBR₃) was compared with a MBBR (**Table**
252 **1**). A 79-day stabilization period at 38°C allowed sufficient acclimatization of the inoculum
253 and, more specifically, biomass growth on the PVA gel carriers of the MBBR. The suspended

254 biomass in the MBBR was gradually wasted during this period, while clear attached growth
255 was observed on the PVA carriers (**Figure S1**). At the start of the actual experiment the
256 settling was excluded to waste all the suspended sludge. This resulted in roughly a doubling
257 of the attached growth (**Figure 2C**) and a further increase of the ammonium removal rate up
258 to $580 \pm 44 \text{ mg N L}^{-1} \text{ d}^{-1}$ (**Figure 2B**). As the SBR₃ sludge content also sharply increased
259 from about 3.3 g VSS L^{-1} (day 6) to 4.5 g VSS L^{-1} (day 16), eventually endangering settling
260 behavior, about one third of the SBR₃ sludge was wasted before the start of the temperature
261 increase. Concurrently, the loading was lowered by one third to prevent overloading, reaching
262 comparable volumetric nitrification rates in both reactors (**Figure 2B**). From day 20 on,
263 temperature was gradually increased in both reactors at a slope of $0.16^\circ\text{C d}^{-1}$ (**Figure 2A**). In
264 accordance with the first reactor experiment, from 38°C to 40°C , no negative effect on the
265 nitrification performance was observed. On the contrary, volumetric rates slightly increased
266 (**Figure 2B**). As temperatures above 40°C initiated reactor failing in the first experiment
267 (**Figure 1**), from 40°C on, the imposed slope was halved to $0.08^\circ\text{C d}^{-1}$ (day 32). At that
268 moment, a technical failure of the pH controller led to acidification (pH 5) in the MBBR
269 resulting in a 18% decrease of nitrification performance. The MBBR recovered, even though
270 temperature further increased. Stable ammonium removal rates of $563 \pm 52 \text{ mg N L}^{-1} \text{ d}^{-1}$
271 (SBR₃) and $358 \pm 40 \text{ mg N L}^{-1} \text{ d}^{-1}$ (MBBR) were observed in both reactors until 45°C . From
272 45.5°C on, however, ammonium removal rates gradually decreased in the MBBR from $358 \pm$
273 40 to $23 \pm 8 \text{ mg N L}^{-1} \text{ d}^{-1}$ at 46.5°C (**Figure 2B**). As more than 90% of the activity was lost,
274 temperature increase was ceased in the MBBR. In contrast, volumetric rates increased in the
275 SBR₃ up to $776 \pm 62 \text{ mg N L}^{-1} \text{ d}^{-1}$ at a temperature as high as 49°C , corresponding with a
276 specific ammonium removal rate of $155 \pm 24 \text{ mg N g VSS}^{-1} \text{ d}^{-1}$ (**Figure 2C**). Nitrite
277 accumulation was observed from temperatures higher than 49°C up to 200 mg N L^{-1} . As batch
278 activity tests with SBR₃ sludge showed that nitrite concentrations up to 500 mg N L^{-1} did not

279 have a significant effect on the ammonium oxidizing activity ($p < 0.05$, **Figure S2**), the loading
280 rate was not adjusted. At 49.5°C, a malfunctioning of the pH controller pump now also
281 acidified the SBR₃ (pH 3-4), resulting in a decrease of ammonium removal activity to 30 mg
282 N L⁻¹ d⁻¹. The temperature in the SBR₃ was decreased to 48.5°C to allow for recovery of the
283 SBR₃. Ammonium oxidation rates increased again reaching >300 mg N L⁻¹ d⁻¹ after 50 days,
284 while nitrite oxidation could not be recovered (**Figure S3**). Overall, the highest temperature
285 where complete and stable nitrification was observed was 45.5°C and 49°C in the MBBR and
286 SBR₃, respectively.

287 **3.2.2. Community adaptation**

288 The adaptive capacity of the SBR₃ and MBBR sludge towards the imposed temperature
289 increase was closely monitored with parallel batch activity tests. Every 2°C along the
290 temperature increase, specific ammonium and nitrite oxidizing activities of both sludge types
291 were measured at the respective reactor temperature and at plus and minus 2°C. The results of
292 these batch activity tests are presented in **Figure 3**. Similar observations were made for both
293 reactors up to 42°C. Although the differences were small, it appeared that between 38 and
294 42°C, the temperature with the highest ammonium oxidizing activity was 40°C. Although the
295 ammonium oxidation optimum in the SBR₃ gradually shifted from 40°C towards 46-48°C
296 (**Figure 3A**), the MBBR optimum did not get higher than 42°C (**Figure 3B**). Moreover, at a
297 reactor temperature of 44°C, no ammonium oxidation activity could be measured in the
298 MBBR sludge at 46°C, clearly predicting the MBBR crash at 46°C (**Figure 3B**). Despite the
299 loss of ammonium oxidation at 46°C, the batch activity test indicates that the MBBR's nitrite
300 oxidizers were still active up to 48°C (**Figure 3D**). The nitrite oxidizers in the SBR₃ seemed
301 to be adapted once the reactor reached 48°C, but a significant inhibition was observed at 50°C
302 (**Figure 3C**). Indeed, temperatures higher than 49°C led to nitrite accumulation in the SBR₃
303 (**Figure 2B**).

305 **3.2.3. Free ammonia sensitivity**

306 Sensitivity of the nitrifying sludge towards elevated free ammonia (FA) was evaluated along
307 the temperature increase. No significant inhibition of ammonium oxidation could be observed
308 in both reactors by FA up to 6 mg N L^{-1} , in contrast, ammonium oxidation was stimulated by
309 elevated FA (**Figure S4 A and B**).

310 The SBR₃'s nitrite oxidizers were only slightly or not inhibited by FA up to 6 mg N L^{-1} at the
311 lower operating temperatures (38-42°C), but were strongly inhibited at 46-48°C with a 50%
312 (IC₅₀) and 100% (IC₁₀₀) inhibitory concentration of 0.67 ± 0.01 and $1.42 \pm 0.08 \text{ mg NH}_3\text{-N L}^{-1}$,
313 respectively (**Figure S4 C**). The opposite trend was observed in the MBBR. Nitrite
314 oxidation was clearly inhibited at 38-40°C, with an IC₅₀ of $0.48 \pm 0.07 \text{ mg NH}_3\text{-N L}^{-1}$, while
315 the inhibition by FA disappeared at elevated temperatures (44-46°C) (**Figure S4 D**), possibly
316 due to an increased diffusion limitation as the biomass concentration in the MBBR, and thus
317 thickness of the biomass, strongly increased over time/temperature.

318 **3.2.4. Sludge production and settleability**

319 The increasing temperature initially induced a sharp decrease in sludge production in the
320 SBR₃. The observed sludge yield halved from 0.074 to $0.035 \text{ g VSS g}^{-1} \text{ N}$ from 38°C to 42°C,
321 whereas it increased again from 44°C to a yield of $0.067 \pm 0.005 \text{ g VSS g}^{-1} \text{ N}$ up to 48°C
322 (**Figure S5**). In contrast, sludge production in the MBBR was equal to $0.11 \text{ g VSS g}^{-1} \text{ N}$ until
323 42°C, whereupon it decreased and finally became negative at 46°C as a result of biomass die
324 off (**Figure 2C**). Settling behavior of the SBR₃ sludge was stable up to 44°C, with a SVI₅ of
325 $241 \pm 38 \text{ mL g}^{-1}$, and improved at 46-48°C with a SVI₅ of $154 \pm 2 \text{ mL g}^{-1}$ (**Figure S5**). The
326 sludge residence time (SRT) in the SBR₃ was 92 ± 7 days, while the SRT of the MBBR was
327 considered infinite as nearly no suspended sludge could be measured in the effluent.

328

329 3.2.5. Functional community analysis

330 The abundance of selected key groups of nitrifying microorganisms was assessed along the
331 temperature increase by means of qPCR. The reactors were inoculated with a subsample of
332 the same inoculum, comprising a relatively well-balanced amount of AOB versus AOA
333 (2.1×10^9 versus 3.5×10^8 *amoA* gene copies g^{-1} VSS) and of the nitrite oxidizers *Nitrospira*
334 spp. versus *Nitrobacter* spp. (6.7×10^9 versus 4.8×10^{10} 16S gene copies g^{-1} VSS). The AOB
335 dominance was preserved in both reactors after the stabilization period reaching an
336 AOB/AOA ratio of 279 and 7091 in the SBR₃ and MBBR, respectively. The bacterial *amoA*
337 gene abundance kept stable up to 45°C at around 10^{10} copies g^{-1} VSS in both reactors, and
338 then gradually decreased (**Figure 2D**). Clear differences in AOA abundances were, however,
339 observed between the different reactors. The MBBR biomass retained significantly less AOA
340 compared with the SBR₃ sludge after the stabilization period (**Figure 2D**, day 16). Moreover,
341 a steep increase in AOA abundance by 3 orders of magnitude was observed in the SBR₃ at
342 about 44°C, rising from 1.0×10^7 to 2.9×10^{10} copies g^{-1} VSS, while the AOA abundance in the
343 MBBR only slightly increased by two orders of magnitude to 8.6×10^8 copies g^{-1} VSS at 46°C.
344 This shows a clear shift in dominant ammonia oxidizers in the SBR₃ from AOB to AOA from
345 45°C on, while this shift never completely occurred in the MBBR. For nitrite oxidation,
346 *Nitrospira* spp. were dominant over *Nitrobacter* spp. in both reactors over the whole
347 experiment (**Figure 2D**). The observed trends in key nitrifier abundances were confirmed by
348 community structure analysis through sequencing of the V5V6 region of the 16S rRNA gene
349 (**Figure S6**). The most dominant AOB retrieved in the MBBR (Phy1) appeared to belong to
350 the *Nitrosomonas europaeae* species (**Figure S7**) and the most dominant AOA in the SBR₃
351 (Phy8) as well as the inoculum (Phy56) belonged to the *Nitrososphaera* genus (**Figure 4**).
352 Interestingly, this AOA (Phy8) only showed a 95% similarity with the AOA initially detected

353 in the inoculum (Phy56). The closest related known NOB of the dominant *Nitrospira* in both
354 reactors is *Nitrospira japonica J1* with 91% similarity (**Figure 5**).

355

356 4. Discussion

357 4.1. Overall performance

358 The adaptive capacities of mesophilic nitrifying sludge over different linear temperature
359 increase patterns and different sludge growth modes were explored in this study of which the
360 main results are summarized in **Table 1**. A non-oscillating temperature pattern (SBR₂)
361 appeared to be more effective than an oscillating pattern (SBR₁) for the tested slope of 0.25°C
362 d⁻¹ as both the volumetric as specific rates were 2-3 times higher. In general, the ‘low-slope’
363 reactors (SBR₃ and MBBR) reached 3 to 30 times higher volumetric rates than the ‘high-
364 slope’ reactors (SBR₁ and SBR₂), at significantly higher temperatures. Finally, the biofilm
365 based system (MBBR) showed 2.5 times lower rates than the parallel floccular growth system
366 (SBR₃). Overall, within the range of the tested parameters/combinations in this study, the
367 highest temperature with moreover the highest volumetric and specific nitrification rates were
368 achieved through the transition of mesophilic nitrifying sludge by a slow, non-oscillating
369 linear temperature increase (SBR₃).

370 The successful transition of the SBR₃ towards thermophilic temperatures was, remarkably,
371 accompanied with a change in observed sludge production (**Figure S5**). The decreasing trend
372 sharply reversed at 44°C finally resulting in comparable observed sludge yields at 38°C and
373 48°C (0.0687 ± 0.005 g VSS g⁻¹ N). It is possible that the temperature window 38-42°C can
374 be considered as sub-optimal for both mesophiles and thermophiles, leading to increased
375 decay rates and/or decreased growth rates, and hence a significantly lower net biomass
376 production. Overall, the observed sludge yields were lower than reported values for
377 combined AOB and NOB sludge yield of 0.19-0.21 g VSS g⁻¹ N at mesophilic temperatures
378 (Barnes and Bliss 1983, Henze et al. 2008). Although shifts in net biomass production, i.e. the
379 observed yield, coincided with the AOA vs. AOB dominance shift in this study, future

380 research should map the underlying biokinetic parameters. Besides growth and decay rate,
381 also the oxygen and nitrogen affinity constants of the respective nitrifiers at different
382 temperatures deserve attention to allow accurate modeling of nitrification at any elevated
383 temperature.

384 In parallel, a clear shift in optimum temperature was observed with the ex-situ activity
385 measurements. These small, fast, high-throughput activity tests, based on simple
386 spectrophotometrical measurements, could predict the loss of ammonium and nitrite oxidation
387 in the MBBR and SBR₃ (**Figure 3**), respectively. One could thus lower the slope of the
388 imposed temperature slope when the optimum does not seem to evolve with the current
389 temperature and so, steer the temperature increase strategy to achieve thermophilic
390 nitrification.

391 **4.2. Temperature increase pattern**

392 Pre-exposure to a certain stress can result in an increased resilience to a secondary exposure
393 (Philippot et al. 2008, Ryall et al. 2012). In the framework of this study, a pre-exposure to an
394 elevated temperature can e.g. induce the production of heat-shock proteins (HSP) that could
395 possibly protect the biomass during a secondary temperature increase and so, improve the
396 adaptive capabilities. This study however showed that the tested oscillating temperature
397 pattern did not improve the adaptive capabilities of mesophilic nitrifying sludge towards
398 higher temperatures (**Figure 1**). The tested amplitude of 2°C was possibly too high to observe
399 beneficial effects and thus, smaller oscillating could eventually give better results.

400 The linear character of the imposed temperature pattern in this study was clearly more
401 successful than stepwise temperature increases reaching only maximum nitrification
402 temperatures of 40 and 42.5°C (Courstens et al. 2014a, Shore et al. 2012). This is in line with
403 observations at a lower temperature range (10-20°C) in which the negative effect of a sudden

404 temperature decrease on nitrification was much stronger than a gradual temperature decrease
405 (Hwang and Oleszkiewicz 2007). Although nitrifiers are known to cope with relatively high
406 seasonal temperature changes in wastewater treatment plants in moderate climates (e.g. 10°C-
407 30°C at DC Water, Washington, USA), this study showed that a relatively low slope in
408 temperature increase was essential to allow the transition of nitrifiers to temperatures higher
409 than 38°C-42°C.

410 **4.3. Sludge growth mode**

411 A floccular growth system (SBR₃) was compared with a biofilm based system (MBBR), as
412 biomass retention of the slow growing autotrophs is essential during the transition process,
413 and could eventually be favored through a biofilm based reactor system. Experiences with
414 thermophilic carbon treatment showed that thermophilic aerobic processes suffer from poor
415 sludge settling properties (Suvilampi and Rintala 2003), thus, operation of settling based
416 system such as a SBR may be threatened. Remarkably, settling behavior of the SBR₃ sludge
417 in this study did not deteriorate (**Figure S5**), resulting in only minor differences in sludge
418 retention time between both reactors.

419 The MBBR was initially hypothesized to better cope with the temperature transition, as
420 biofilms show increased resistance to many types of environmental challenges (Gilbert et al.
421 2002). Recently, Gilbert et al. (2015) showed that nitrate production in a partial
422 nitritation/anammox MBBR was more resilient against a gradual temperature reduction (20°C
423 to 10°C, 0.07 °C d⁻¹), compared with a SBR, though ammonium oxidation declined similarly
424 in both reactor types. Several observations, such as the increased resistance of biofilms
425 towards antibiotics, are mainly explained by the restricted diffusion (Mah and O'Toole 2001).
426 Recently, other factors, such as slow growth rate, high culture density and heterogeneity, were
427 shown to influence the general stress response in biofilms (Mah and O'Toole 2001, Ryall et

428 al. 2012), and could eventually favor the adaptive capacities of nitrifiers towards elevated
429 temperatures. This study is however in contrast with this hypothesis, as the ammonium
430 oxidation MBBR failed around 46°C, while it could still be maintained until 49°C in the
431 SBR₃ (**Figure 2B**). The successful transition in the SBR₃ seemed to be related to the observed
432 shift of AOB to AOA dominance that was not completely achieved in the MBBR (**Figure**
433 **2D**). This is in accordance with literature, where most described thermophilic ammonium
434 oxidizers are archaeal (de la Torre et al. 2008, Hatzepichler et al. 2008, Lebedeva et al.
435 2013). The slower growth rate of the nitrifiers in the MBBR, initially supposed to favor the
436 general stress response on a short term (Ryall et al. 2012), probably delayed the essential
437 selection process on a long term. Indeed, an increase in AOA abundance in the biofilm was
438 also observed, though one month later than in the SBR₃ (**Figure 2D**). Furthermore, although
439 both reactors were inoculated with the same AOA/AOB ratio, the relative decrease in AOA
440 during the stabilization period was more pronounced in the biofilm than in the flocs resulting
441 in an initially lower AOA abundance in the biofilm. The late start of the increasing trend of
442 AOA in the MBBR suggests that the essential shift could eventually also have been achieved
443 with an even lower slope of temperature increase. Potentially a stronger selection for fast
444 growing micro-organisms was made in the MBBR versus the SBR giving more advantage to
445 the faster growing AOB. Another possible reason for the differential stimulation of AOA vs.
446 AOB in both systems might be the levels and dynamics of DO and NH₄⁺ concentrations, as
447 key substrates for ammonia oxidation and potentially niche differentiation. Figure S8 displays
448 the typical concentration profiles, highlighting more frequent fluctuations of the bulk
449 concentrations of both substrates along with lower concentrations of NH₄⁺ in the SBR
450 compared to the MBBR, possibly favoring AOA stimulation. Future research should focus on
451 the actual substrate availability for the ammonia oxidizers within the flocs versus biofilm.

452 Besides the actual abundance of AOA in the biofilm, different, less thermotolerant, AOA
453 species could have been enriched in the biofilm, compared with the floccular sludge.

454 Observations regarding nitrite oxidation were in line with literature, stating that *Nitrospira* is
455 the most dominant nitrite oxidizer up to 60°C (Edwards et al. 2013, Lebedeva et al. 2011,
456 Marks et al. 2012). In this study, no shifts were observed, and *Nitrospira* was dominant in
457 both reactors over the entire experiment (**Figure 2D**). However, remarkable differences in
458 free ammonia sensitivity were observed between reactors and over time (**Figure S4**),
459 suggesting that a possible selection on strain level occurred during the transition. Overall,
460 nitrite oxidizers were much more sensitive compared with the ammonium oxidizers, finally
461 resulting in the development of a partial nitrification reactor at 48.5°C, opening opportunities
462 for short-cut nitrogen removal processes.

463 **4.4. Practical implications**

464 The results of this study suggest that existing mesophilic nitrifying wastewater plants can be
465 upgraded to thermophilic systems through a slow, non-oscillating linear temperature increase.
466 Excluding the stabilization period, which is non-relevant for existing plants, this could be
467 achieved in about 140 days. Close monitoring of the transition by high-throughput activity
468 tests as described in this study, could moreover allow an even faster transition period. It
469 should be emphasized that, beside the temperature increase pattern, the presence of AOA in
470 the mesophilic sludge appeared to be essential for a successful transition. The fact that AOA
471 appear to be distributed in wastewater treatment plants worldwide, even in equal or higher
472 abundance than AOB (Limpiyakorn et al. 2013), opens thus opportunities for thermophilic
473 nitrogen removal.

474

475 **5. Conclusions**

- 476 • The oscillating temperature pattern with an amplitude of 2°C and a slope of 0.25°C d⁻¹
477 achieved a low nitrification rate of 26 ± 5 mg N L⁻¹ d⁻¹ at 42°C and lost all activity at
478 45°C.
- 479 • The moving bed biofilm reactor subjected to a slope of 0.08-0.16°C d⁻¹ was able to
480 oxidize ammonium up to 46°C, though, at a low volumetric rate of 32 ± 7 mg N L⁻¹ d⁻¹
481 .
- 482 • Nitrification rates of up to 800 mg N L⁻¹ d⁻¹ and 170 mg N g VSS⁻¹ d⁻¹ were achieved
483 at 49°C through gradual adaptation (0.08 °C d⁻¹) of mesophilic nitrifying sludge in
484 suspension (SBR₃).
- 485 • The successful transition from mesophilic to thermophilic ammonia oxidation in SBR₃
486 was linked to a dominance shift of archaeal above bacterial ammonia oxidizers.
- 487 • Ex-situ batch activity measurements can serve as a good tool to monitor the process
488 response to transition, predicting reactor failures, thus enabling steering of the
489 temperature increase pattern.

490

491 **Acknowledgements**

492 E.N.P.C and S.E.V. were supported as doctoral candidate (Aspirant) and postdoctoral fellow,
493 respectively, by the Research Foundation Flanders (FWO-Vlaanderen). R.V.V. was supported
494 as a postdoctoral fellow from the Belgian Science Policy Office (BELSPO). The reactor
495 equipment used for this study was by the King Baudouin Foundation. We thank José M.
496 Carvajal-Arroyo for the assistance with the reactor experiment and Jo De Vrieze for the
497 scientific discussions.

- 499 Barnes, D. and Bliss, P.J. (1983) Biological control of nitrogen in wastewater treatment, E. & F.N.
500 Spon, London.
- 501 Bohorquez, L.C., Delgado-Serrano, L., Lopez, G., Osorio-Forero, C., Klepac-Ceraj, V., Kolter, R.,
502 Junca, H., Baena, S. and Mercedes Zambrano, M. (2012) In-depth Characterization via
503 Complementing Culture-Independent Approaches of the Microbial Community in an
504 Acidic Hot Spring of the Colombian Andes. *Microbial Ecology* 63(1), 103-115.
- 505 Camargo, J.A. and Alonso, A. (2006) Ecological and toxicological effects of inorganic nitrogen
506 pollution in aquatic ecosystems: A global assessment. *Environment International* 32(6),
507 831-849.
- 508 Camarinha-Silva, A., Jáuregui, R., Chaves-Moreno, D., Oxley, A.P.A., Schaumburg, F., Becker, K.,
509 Wos-Oxley, M.L. and Pieper, D.H. (2014) Comparing the anterior nare bacterial
510 community of two discrete human populations using Illumina amplicon sequencing.
511 *Environmental Microbiology* 16(9), 2939-2952.
- 512 Cole, J.R., Wang, Q., Fish, J.A., Chai, B., McGarrell, D.M., Sun, Y., Brown, C.T., Porras-Alfaro, A.,
513 Kuske, C.R. and Tiedje, J.M. (2014) Ribosomal Database Project: data and tools for high
514 throughput rRNA analysis. *Nucleic Acids Res* 42(Database issue), D633-642.
- 515 Courtens, E.N.P., Boon, N., De Schryver, P. and Vlaeminck, S.E. (2014a) Increased salinity
516 improves the thermotolerance of mesophilic nitrification. *Applied Microbiology and*
517 *Biotechnology* 98(10), 4691-4699.
- 518 Courtens, E.N.P., Vlaeminck, S.E., Vilchez-Vargas, R., Verliefde, A., Jauregui, R., Pieper, D.H. and
519 Boon, N. (2014b) Trade-off between mesophilic and thermophilic denitrification: Rates
520 vs. sludge production, settleability and stability. *Water Research* 63, 234-244.
- 521 de la Torre, J.R., Walker, C.B., Ingalls, A.E., Konneke, M. and Stahl, D.A. (2008) Cultivation of a
522 thermophilic ammonia oxidizing archaeon synthesizing crenarchaeol. *Environmental*
523 *Microbiology* 10(3), 810-818.
- 524 Edwards, T.A., Calica, N.A., Huang, D.A., Manoharan, N., Hou, W., Huang, L., Panosyan, H., Dong, H.
525 and Hedlund, B.P. (2013) Cultivation and characterization of thermophilic *Nitrospira*
526 species from geothermal springs in the US Great Basin, China, and Armenia. *FEMS*
527 *Microbiol Ecol* 85(2), 283-292.
- 528 Erisman, J.W., Sutton, M.A., Galloway, J., Klimont, Z. and Winiwarter, W. (2008) How a century of
529 ammonia synthesis changed the world. *Nature Geoscience* 1(10), 636-639.
- 530 Galloway, J.N., Winiwarter, W., Leip, A., Leach, A.M., Bleeker, A. and Erisman, J.W. (2014)
531 Nitrogen footprints: past, present and future. *Environmental Research Letters* 9(11).
- 532 Gilbert, E.M., Agrawal, S., Schwartz, T., Horn, H. and Lackner, S. (2015) Comparing different
533 reactor configurations for Partial Nitrification/Anammox at low temperatures. *Water*
534 *Research* 81(0), 92-100.
- 535 Gilbert, P., Maira-Litran, T., McBain, A.J., Rickard, A.H. and Whyte, F.W. (2002) *Advances in*
536 *Microbial Physiology*, pp. 203-256, Academic Press.
- 537 Greenberg, A.E., Clesceri, L.S. and Eaton, A.D. (1992) *Standard Methods for the Examination of*
538 *Water and Wastewater*, American Public Health Association, Washington DC.
- 539 Hatzenpichler, R., Lebedeva, E.V., Spieck, E., Stoecker, K., Richter, A., Daims, H. and Wagner, M.
540 (2008) A moderately thermophilic ammonia-oxidizing crenarchaeote from a hot spring.
541 *Proceedings of the National Academy of Sciences of the United States of America* 105(6),
542 2134-2139.
- 543 Henze, M., Van Loosdrecht, M., Ekama, G. and Brdjanovic, D. (2008) *Biological Wastewater*
544 *Treatment: Principles, Modelling and Design*, IWA Publishing, London.
- 545 Hwang, J.H. and Oleszkiewicz, J.A. (2007) Effect of cold-temperature shock on nitrification. *Water*
546 *Environ Res* 79(9), 964-968.
- 547 Kuai, L.P. and Verstraete, W. (1998) Ammonium removal by the oxygen-limited autotrophic
548 nitrification-denitrification system. *Applied and Environmental Microbiology* 64(11),
549 4500-4506.

550 Lackner, S., Gilbert, E.M., Vlaeminck, S.E., Joss, A., Horn, H. and van Loosdrecht, M.C.M. (2014)
551 Full-scale partial nitrification/anammox experiences - An application survey. *Water*
552 *Research* 55, 292-303.

553 Lapara, T.M. and Alleman, J.E. (1999) Thermophilic aerobic biological wastewater treatment.
554 *Water Research* 33(4), 895-908.

555 Lebedeva, E.V., Hatzepichler, R., Pelletier, E., Schuster, N., Hauzmayer, S., Bulaev, A., Grigor'eva,
556 N.V., Galushko, A., Schmid, M., Palatinszky, M., Le Paslier, D., Daims, H. and Wagner, M.
557 (2013) Enrichment and Genome Sequence of the Group I. 1a Ammonia-Oxidizing
558 Archaeon "Ca. Nitrosotenuis uzonensis" Representing a Clade Globally Distributed in
559 Thermal Habitats. *Plos One* 8(11).

560 Lebedeva, E.V., Off, S., Zumbraegel, S., Kruse, M., Shagzhina, A., Luecker, S., Maixner, F., Lipski, A.,
561 Daims, H. and Spieck, E. (2011) Isolation and characterization of a moderately
562 thermophilic nitrite-oxidizing bacterium from a geothermal spring. *Fems Microbiology*
563 *Ecology* 75(2), 195-204.

564 Li, J., Zheng, Y.-M., Liu, Y.-R., Ma, Y.-B., Hu, H.-W. and He, J.Z. (2014) Initial Copper Stress
565 Strengthens the Resistance of Soil Microorganisms to a Subsequent Copper Stress.
566 *Microbial Ecology* 67(4), 931-941.

567 Limpiyakorn, T., Fuerhacker, M., Haberl, R., Chodanon, T., Srithep, P. and Sonthiphand, P. (2013)
568 amoA-encoding archaea in wastewater treatment plants: a review. *Applied Microbiology*
569 *and Biotechnology* 97(4), 1425-1439.

570 Lopez-Vazquez, C.M., Kubare, M., Saroj, D.P., Chikamba, C., Schwarz, J., Daims, H. and Brdjanovic,
571 D. (2014) Thermophilic biological nitrogen removal in industrial wastewater treatment.
572 *Applied Microbiology and Biotechnology* 98(2), 945-956.

573 Lowry, O.H., Rosebrough, N.J., Farr, A.L. and Randall, R.J. (1951) Protein measurement with the
574 Folin phenol reagent. *J Biol Chem* 193(1), 265-275.

575 Mah, T.F. and O'Toole, G.A. (2001) Mechanisms of biofilm resistance to antimicrobial agents.
576 *Trends in Microbiol* 9(1), 34-39.

577 Marks, C.R., Stevenson, B.S., Rudd, S. and Lawson, P.A. (2012) Nitrospira-dominated biofilm
578 within a thermal artesian spring: a case for nitrification-driven primary production in a
579 geothermal setting. *Geobiology* 10(5), 457-466.

580 Philippot, L., Cregut, M., Cheneby, D., Bressan, M., Dequiet, S., Martin-Laurent, F., Ranjard, L. and
581 Lemanceau, P. (2008) Effect of primary mild stresses on resilience and resistance of the
582 nitrate reducer community to a subsequent severe stress. *Fems Microbiology Letters*
583 285(1), 51-57.

584 Ryall, B., Eydallin, G. and Ferenci, T. (2012) Culture history and population heterogeneity as
585 determinants of bacterial adaptation: the adaptomics of a single environmental
586 transition. *Microbiol Mol Biol Rev* 76(3), 597-625.

587 Schloss, P.D., Westcott, S.L., Ryabin, T., Hall, J.R., Hartmann, M., Hollister, E.B., Lesniewski, R.A.,
588 Oakley, B.B., Parks, D.H., Robinson, C.J., Sahl, J.W., Stres, B., Thallinger, G.G., Van Horn, D.J.
589 and Weber, C.F. (2009) Introducing mothur: open-source, platform-independent,
590 community-supported software for describing and comparing microbial communities.
591 *Appl Environ Microbiol* 75(23), 7537-7541.

592 Shore, J.L., M'Coy, W.S., Gunsch, C.K. and Deshusses, M.A. (2012) Application of a moving bed
593 biofilm reactor for tertiary ammonia treatment in high temperature industrial
594 wastewater. *Bioresource Technology* 112, 51-60.

595 Suvilampi, J. and Rintala, J. (2003) Thermophilic aerobic wastewater treatment, process
596 performance, biomass characteristics, and effluent quality. *Reviews in Environmental*
597 *Science and Biotechnology* 2(1), 35-51.

598 Tamura, K., Peterson, D., Peterson, N., Stecher, G., Nei, M. and Kumar, S. (2011) MEGA5:
599 Molecular Evolutionary Genetics Analysis Using Maximum Likelihood, Evolutionary
600 Distance, and Maximum Parsimony Methods. *Molecular Biology and Evolution* 28(10),
601 2731-2739.

- 602 Treusch, A.H., Leininger, S., Kletzin, A., Schuster, S.C., Klenk, H.P. and Schleper, C. (2005) Novel
603 genes for nitrite reductase and Amo-related proteins indicate a role of uncultivated
604 mesophilic crenarchaeota in nitrogen cycling. *Environ Microbiol* 7(12), 1985-1995.
- 605 Vilchez-Vargas, R., Geffers, R., Suarez-Diez, M., Conte, I., Waliczek, A., Kaser, V.S., Kralova, M.,
606 Junca, H. and Pieper, D.H. (2013) Analysis of the microbial gene landscape and
607 transcriptome for aromatic pollutants and alkane degradation using a novel internally
608 calibrated microarray system. *Environmental Microbiology* 15(4), 1016-1039.
- 609 Vlaeminck, S.E., De Clippeleir, H. and Verstraete, W. (2012) Microbial resource management of
610 one-stage partial nitritation/anammox. *Microbial Biotechnology* 5(3), 433-448.
- 611 Windey, K., De Bo, I. and Verstraete, W. (2005) Oxygen-limited autotrophic nitrification-
612 denitrification (OLAND) in a rotating biological contactor treating high-salinity
613 wastewater. *Water Research* 39(18), 4512-4520.

614

615 **Table and Figure captions**

616 **Table 1.** Overview of reactor parameters, temperature increase patterns, volumetric and
617 biomass specific rates achieved at the highest temperature where complete nitrification was
618 observed in the two different reactor experiments. Averages calculated over at least 3
619 hydraulic retention times (± 3 operation days). n.a.: not applicable, SBR: sequencing batch
620 reactor, MBBR: moving bed biofilm reactor, VER: volumetric exchange ratio, HRT:
621 hydraulic retention time.

622

623 **Figure 1.** Temperature increase pattern **(A)** and nitrifying reactor performance **(B)** of two
624 sequential batch reactors comparing a linear with an oscillating temperature increase (0.25°C
625 d^{-1}).

626 **Figure 2.** Operation and performance characteristics of SBR₃ (left) and MBBR (right). **(A)**
627 Temperature increase patterns. **(B)** Volumetric ammonium removal and nitrite/nitrate
628 production rates. **(C)** Specific rates (left axis) and sludge content (right axis). **(D)** Abundance
629 of nitrifiers as determined by qPCR.

630 **Figure 3.** Relative temperature activity curves for ammonium **(A,B)** and nitrite **(C,D)**
631 oxidation of the SBR₃ **(A,C)** and MBBR **(B,D)** sludge. Each color curve represents a batch
632 test performed at a certain reactor temperature, of which the temperature is indicated with a
633 symbol. Per batch test, the temperature where the highest activity was measured was indicated
634 as the 'optimum temperature' and assigned as 100%. All experiments were performed in
635 sextuple, and statistically significant optima (student's t-test, $p < 0.05$) are indicated with an
636 asterisk.

637 **Figure 4.** Phylogenetic relationships between the most dominant archaeal 16S rRNA gene
638 sequences in the SBR₃ reactor (Phy8) and the inoculum used (Phy56) and all described AOA

639 cultures or isolates, as well as relevant environmental clone sequences. Phy7 refers to the
640 archaeal 16S rRNA gene sequence detected in the thermophilic nitrifying reactor enriched
641 from compost by Courtens et al. (*Under review*).

642 **Figure 5.** Phylogenetic relationships between the most dominant *Nitrospira* 16S rRNA gene
643 sequence in the SBR₃ and MBBR (Phy3) and all described *Nitrospira* cultures or isolates, as
644 well as relevant environmental clone sequences. Phy1 refers to the *Nitrospira* 16S rRNA gene
645 sequence detected in the thermophilic nitrifying reactor enriched from compost by Courtens et
646 al. (*Under review*).

Table 1[Click here to download Table: Table 1.docx](#)

Table 1. Overview of reactor parameters, temperature increase patterns, volumetric and biomass specific rates achieved at the highest temperature where complete nitrification was observed in the two different reactor experiments. Averages calculated over at least 3 hydraulic retention times (± 3 operation days). n.a.: not applicable, SBR: sequencing batch reactor, MBBR: moving bed biofilm reactor, VER: volumetric exchange ratio, HRT: hydraulic retention time.

Reactor(type)	Experiment 1		Experiment 2	
	SBR ₁	SBR ₂	SBR ₃	MBBR
Linear temperature increase	Oscillating	Steady	Steady	
Linear slope ($^{\circ}\text{C d}^{-1}$)	0.25		<40 $^{\circ}\text{C}$: 0.16 >40 $^{\circ}\text{C}$: 0.08	
Oscillating amplitude ($^{\circ}\text{C}$)	2	n.a.	n.a.	
Oscillating frequency (d^{-1})	0.088	n.a.	n.a.	
Experimental periods				
Stabilization (d)	7		79	
Temperature increase (d)	50		150	
VER (%)	25		20	
Cycle duration (h)	6		4	
Flowrate (L)	2.1 ± 0.2		2.1 ± 0.3	
HRT (d)	1.0 ± 0.2		1.0 ± 0.2	
Highest temperature ($^{\circ}\text{C}$)	42	42	49	45.5
Ammonium conversion rates*				
Volumetric ($\text{mg N L}^{-1} \text{d}^{-1}$)	26 ± 5	90 ± 3	794 ± 57	309 ± 30
Specific ($\text{mg N g}^{-1} \text{VSS d}^{-1}$)	72**	139 ± 18	151 ± 7	67**

* In all cases, nitrite accumulation was negligible and nitrate formation > 90% of ammonium removal

** Only one biomass measurement available for the specific period

Figure 1
[Click here to download high resolution image](#)

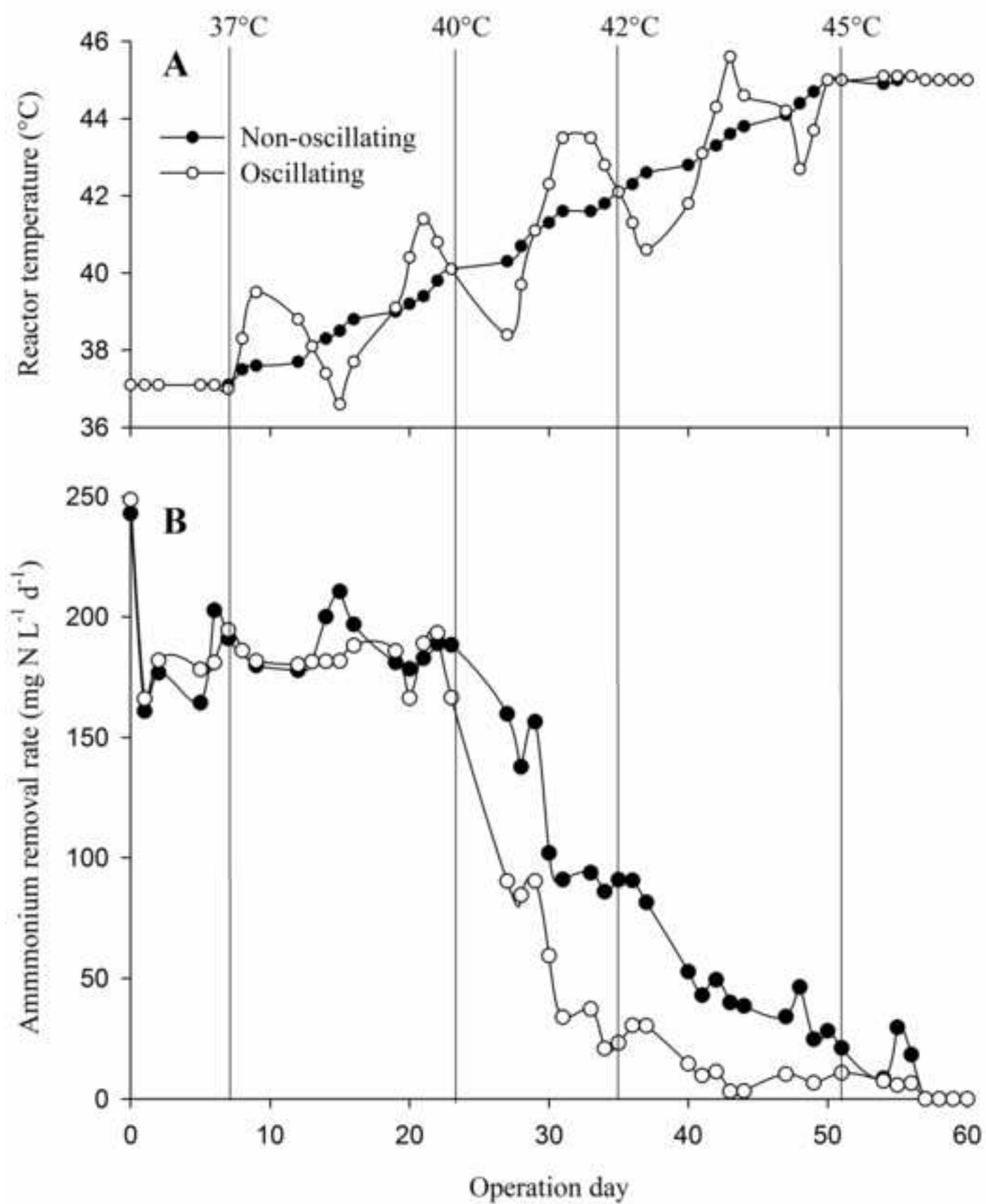


Figure 2
[Click here to download high resolution image](#)

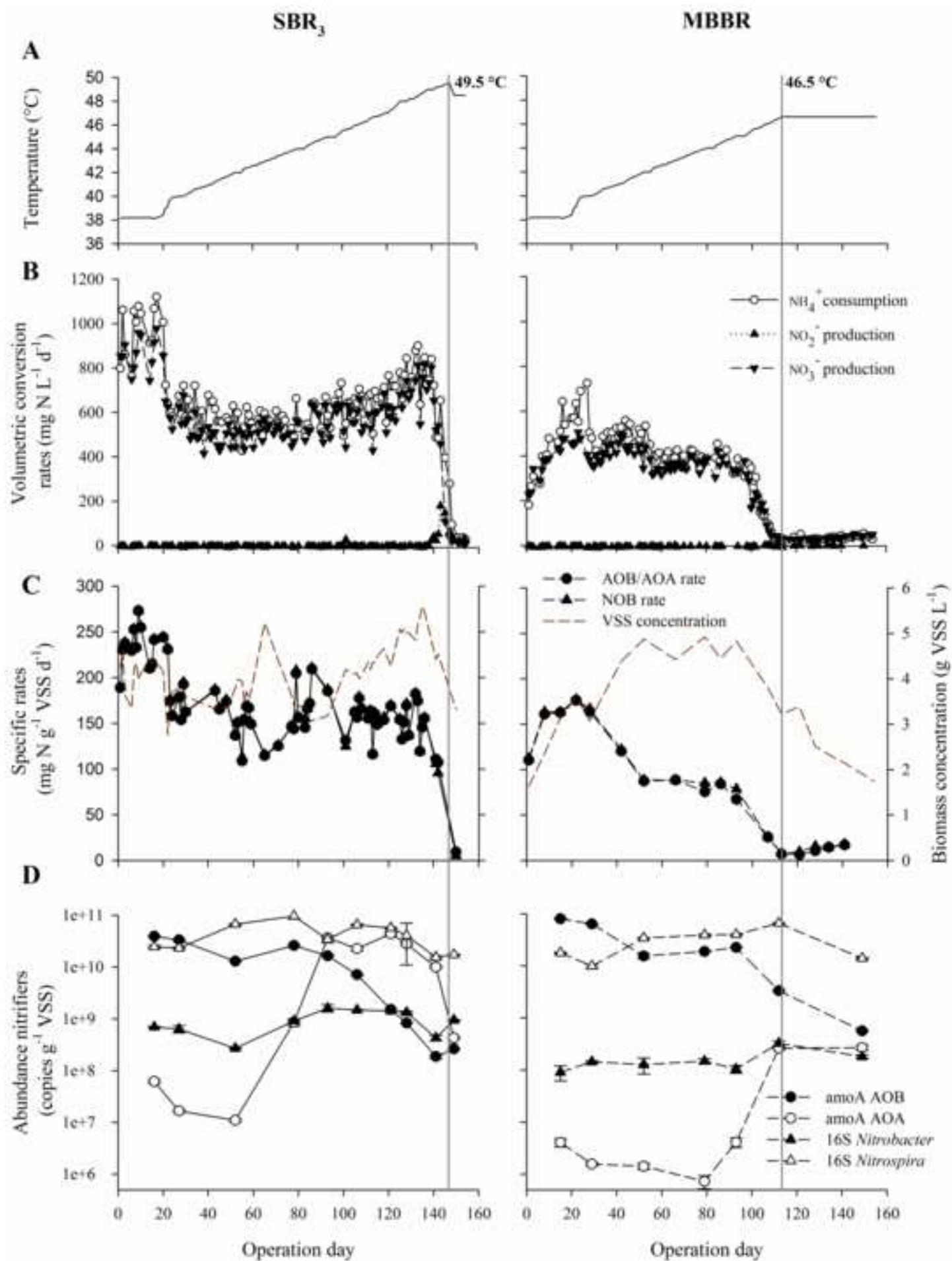


Figure 3
[Click here to download high resolution image](#)

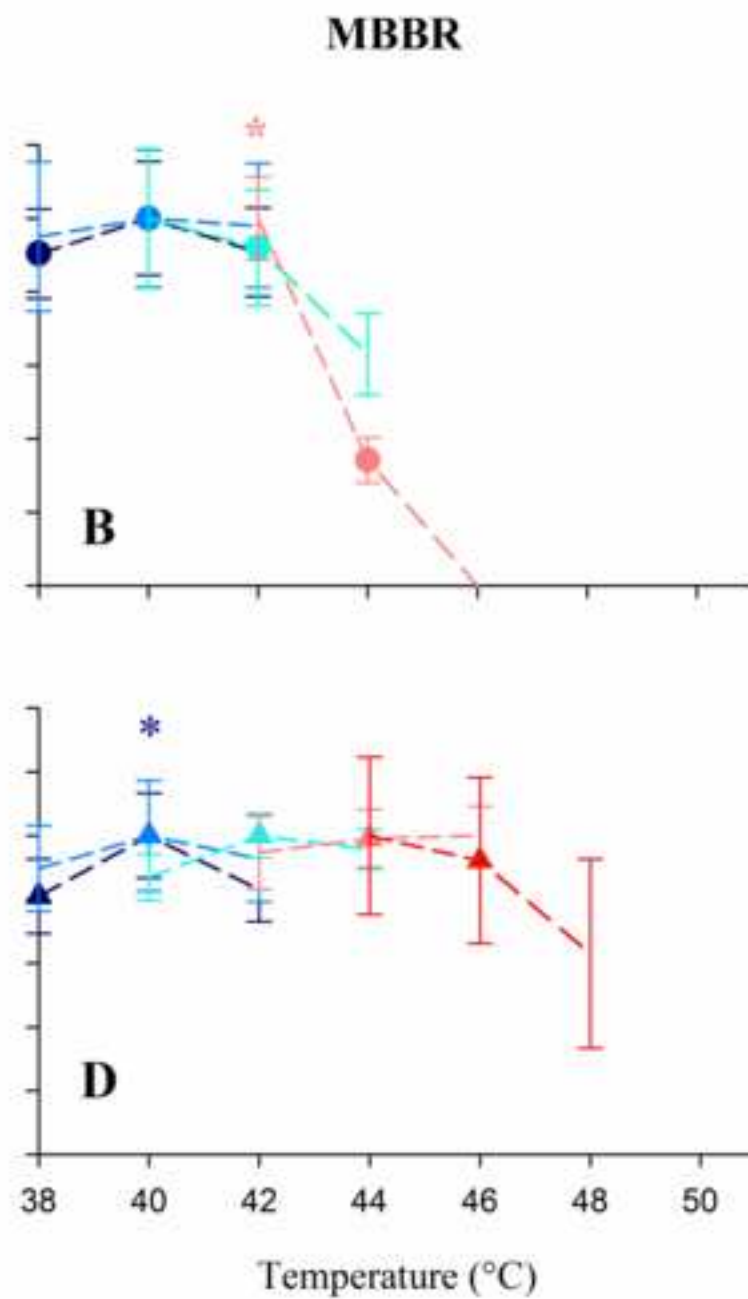
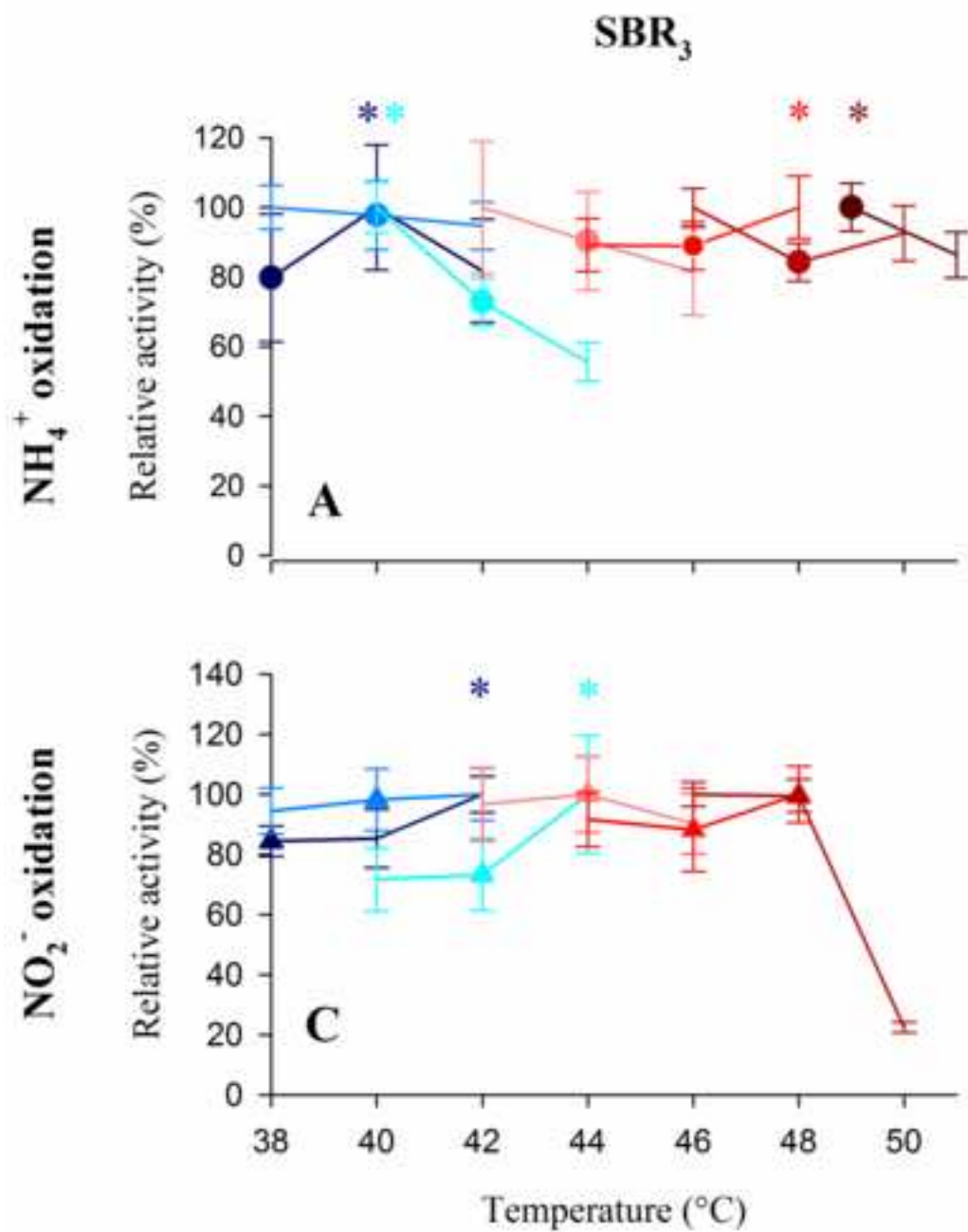


Figure 4

[Click here to download high resolution image](#)

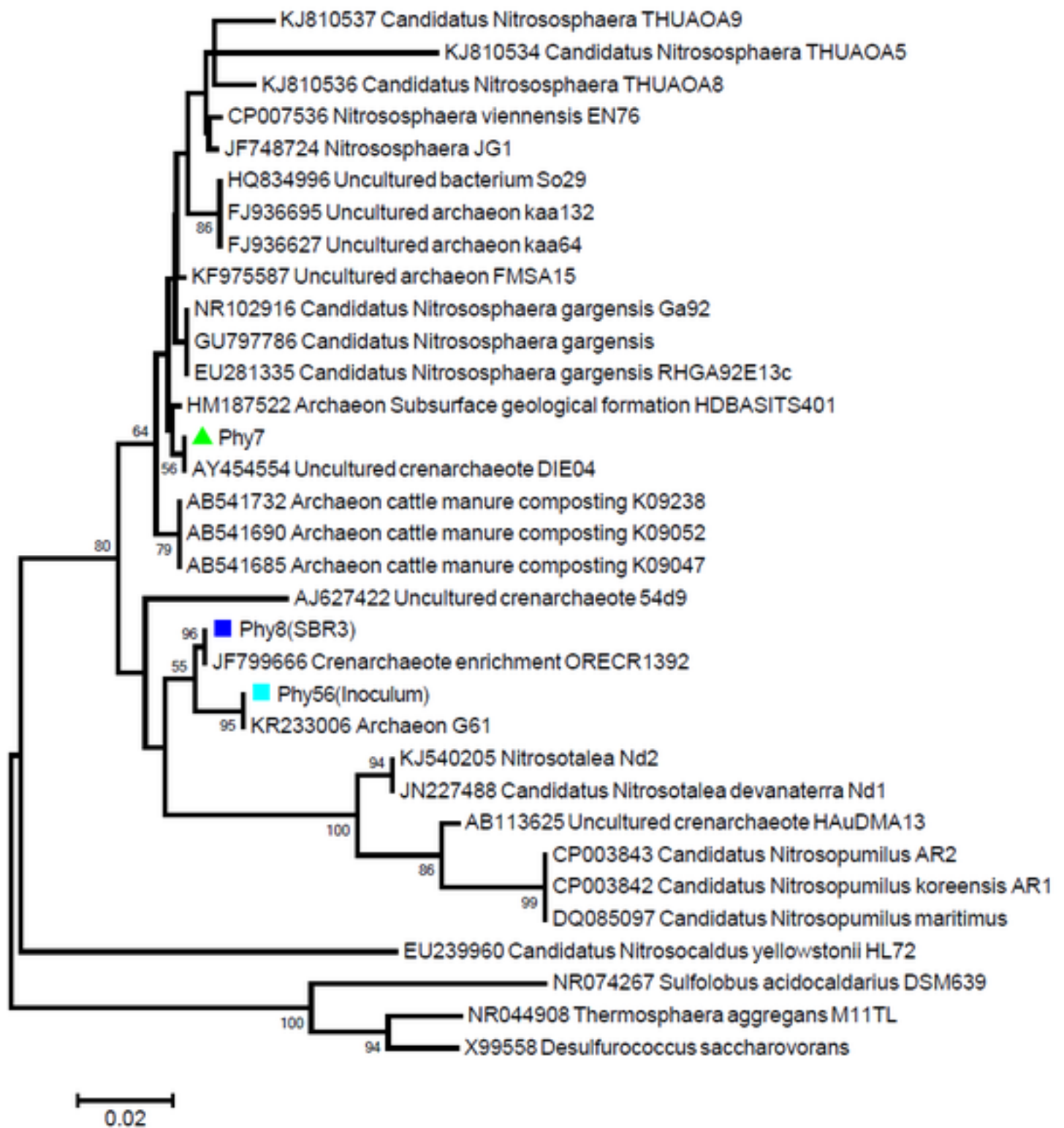


Figure 5
[Click here to download high resolution image](#)

